Centrum voor Wiskunde en Informatica

REPORTRAPPORT

MAS

Modelling, Analysis and Simulation

Modelling, Analysis and Simulation

Stability of negative ionization fronts: regularization by electric screening?

M. Arrayas, U. Ebert

REPORT MAS-E0313 SEPTEMBER 02, 2003

CWI is the National Research Institute for Mathematics and Computer Science. It is sponsored by the Netherlands Organization for Scientific Research (NWO).
CWI is a founding member of ERCIM, the European Research Consortium for Informatics and Mathematics.

CWI's research has a theme-oriented structure and is grouped into four clusters. Listed below are the names of the clusters and in parentheses their acronyms.

Probability, Networks and Algorithms (PNA)

Software Engineering (SEN)

Modelling, Analysis and Simulation (MAS)

Information Systems (INS)

P.O. Box 94079, 1090 GB Amsterdam (NL)
Kruislaan 413, 1098 SJ Amsterdam (NL)
Telephone +31 20 592 9333
Telefax +31 20 592 4199

ISSN 1386-3703

Stability of negative ionization fronts: regularization by electric screening?

ABSTRACT

We recently have proposed that a reduced interfacial model for streamer propagation is able to explain spontaneous branching. Such models require regularization. In the present paper we investigate how transversal Fourier modes of a planar ionization front are regularized by the electric screening length. For a fixed value of the electric field ahead of the front we calculate the dispersion relation numerically. These results guide the derivation of analytical asymptotes for arbitrary fields: for small wave-vector k, the growth rate s(k) grows linearly with k, for large k, it saturates at some positive plateau value. We include a physical interpretation of these results.

2000 Mathematics Subject Classification: 35P15, 35L67, 82D10

Keywords and Phrases: stability analysis; nonlinear ionization waves; shock fronts; streamer discharges

Stability of negative ionization fronts: regularization by electric screening?

Manuel Arrayás[1,2] and Ute Ebert[2,3]
[1] Universidad Rey Juan Carlos, Dept. de Física, Tulipán s/n, 28933, Móstoles, Madrid, Spain,
[2] CWI, P.O.Box 94079, 1090 GB Amsterdam, The Netherlands, and
[3] Dept. Physics, Eindhoven Univ. Techn., The Netherlands.

(Dated: July 22, 2003)

We recently have proposed that a reduced interfacial model for streamer propagation is able to explain spontaneous branching. Such models require regularization. In the present paper we investigate how transversal Fourier modes of a planar ionization front are regularized by the electric screening length. For a fixed value of the electric field ahead of the front we calculate the dispersion relation numerically. These results guide the derivation of analytical asymptotes for arbitrary fields: for small wave-vector k, the growth rate $s(k)$ grows linearly with k, for large k, it saturates at some positive plateau value. We include a physical interpretation of these results.

I. INTRODUCTION

Streamers generically appear in electric breakdown when a sufficiently high voltage is suddenly applied to a medium with low or vanishing conductivity. They consist of extending fingers of ionized matter and are ubiquitous in nature and technology. Frequently they are observed to branch [1, 2]. There is a traditional qualitative concept for streamer branching based on rare photo-ionization events [3, 4, 5, 6, 7]. However, our recent work [8, 9, 10] has shown that even the simplest, fully deterministic streamer model without photo-ionization can exhibit branching. In particular, we have proposed [8] that a streamer approaching the Lozansky-Firsov limit of ideal conductivity [11] can branch spontaneously due to a Laplacian interfacial instability [12]. This mechanism is quite different from the one proposed previously. It requires less microscopic physical interaction mechanisms, but is based on a dynamically evolving internal interfacial structure of the propagating streamer head. Analytical branching predictions from the simplest type of interfacial approximation can be found in [10].

However, the simple interfacial model investigated in [10] requires regularization to prevent the formation of cusps. The nature of this regularization has to be derived from the underlying gas discharge physics; it recently has been subject of debate [13, 14]. We argue that one regularization mechanism is generically inherent in any discharge model, namely the thickness of the electric screening layer. This is the subject of the present paper: we study how the electric screening layer present in the partial differential equations of the electric discharge influences the stability of an ionization front, correcting the simple interfacial model proposed in [8, 11, 12, 15] and solved in [10]. To be precise, we derive the dispersion relation for transversal Fourier-modes of a planar ionization front. We treat a negative front in a model as in [8, 9, 12, 15, 16, 17]. We neglect diffusion and assume propagation into a completely non-ionized state; therefore the front has a discontinuity where the electron density jumps from zero to a finite height. Diffusion is neglected to prevent the mathematical challenges associated with pulled fronts [18, 19]. In turn we have to analyze discontinuous fronts.

Here we anticipate the result of the paper: if the field far ahead of a planar negative ionization front is E_∞, then a transversal Fourier perturbation with wave vector k grows with rate

$$s(k) = \begin{cases} |E_\infty|k & \text{for } k \ll \alpha(E_\infty) \\ |E_\infty|\alpha(E_\infty)/2 & \text{for } k \gg \alpha(E_\infty) \end{cases} , \qquad (1)$$

where $\alpha(E)$ is the effective impact ionization coefficient within a local field E; α sets the size of the inverse electric screening length. The behavior for large k is a correction to the interfacial model treated in [10]; in that model we would have $s(k) = |E_\infty|k$ for all k. The result (1) had been quoted already in [8, 15], however, without derivation. This derivation and the consecutive physical insight are the content of the present paper.

In detail, the paper is organized as follows: in Sec. II we summarize the minimal streamer model in the limit of vanishing diffusion and recall multiplicity, selection and analytical form of uniformly translating planar front solutions; we then derive the asymptotic behavior at the position of the shock and far behind the shock, and we discuss two degeneracies of the problem. In Sec. III we set up the framework of the linear perturbation analysis for transversal Fourier modes, first the equation of motion and then the boundary conditions and the solution strategy. In Sect. IV we present numerical results for the dispersion relation for field $E_\infty = -1$, and we derive the asymptotes (1) analytically for arbitrary E_∞. The small k limit is related to one of the degeneracies of the unperturbed problem, for the large k limit we also present a physical interpretation. Sect. V contains conclusions and outlook.

II. MINIMAL STREAMER MODEL AND PLANAR FRONT SOLUTIONS

A. The minimal model

We investigate the minimal streamer model, i.e., a "fluid approximation" with local field-dependent impact ionization reaction in a non-attaching gas like argon or nitrogen [8, 9, 12, 15, 16, 17, 20]. For physical parameters and dimensional analysis, we refer to our previous discussions in [8, 9, 12, 15]. When diffusion is neglected, the dimensionless model has the form

$$\partial_t \sigma \;-\; \nabla\cdot(\sigma\,\mathbf{E}) \;=\; \sigma\, f(\mathbf{E})\;, \tag{2}$$

$$\partial_t \rho \;=\; \sigma\, f(\mathbf{E})\;, \tag{3}$$

$$\nabla\cdot\mathbf{E} \;=\; \rho-\sigma \quad,\quad \mathbf{E}=-\nabla\phi\;, \tag{4}$$

where σ is the electron and ρ the ion density and $\mathbf{E}$ the electric field. Here the electron current is assumed to be $\sigma\mathbf{E}$, and the ion current is neglected. Electron–ion pairs are assumed to be generated with rate $\sigma f(\mathbf{E}) = \sigma|\mathbf{E}|\ \alpha(|\mathbf{E}|)$ where $\sigma|\mathbf{E}|$ is the absolute value of electron current and $\alpha(\mathbf{E})$ the effective impact ionization cross section within a field $\mathbf{E}$. Hence $f(\mathbf{E})$ is

$$f(\mathbf{E}) = |\mathbf{E}|\ \alpha(|\mathbf{E}|)\ . \tag{5}$$

For numerical calculations, we use the Townsend approximation

$$\alpha(|\mathbf{E}|) = e^{-1/|\mathbf{E}|}. \tag{6}$$

For analytical calculations, an arbitrary function $\alpha(\mathbf{E})$ can be chosen where we only assume that

$$f(\mathbf{E}) = f(|\mathbf{E}|) \quad \text{and} \quad \alpha(0)=0\ . \tag{7}$$

The last identity entails that $f(0) = 0 = f'(0)$. For certain results we also need that $\alpha(|\mathbf{E}|)$ does not decrease when $|\mathbf{E}|$ increases, hence that $\alpha' \geq 0$.

Note that the electrons are the only mobile species, and they are also creating additional ionization, while ions ρ and electric potential ϕ or field $\mathbf{E}$ follow the dynamics of the electron density σ, and couple back onto it.

B. Uniformly translating ionization fronts: multiplicity and dynamical selection

We now recall essential properties of uniformly translating planar fronts that can be constructed for appropriate boundary conditions. Particular fronts are selected by the initial conditions.

First of all, a constant mode of propagation requires a planar particle distribution that we assume to vary only in the z direction: $(\sigma,\rho) = (\sigma(z,t),\rho(z,t))$; the particle densities for large positive z are assumed to vanish. The field far ahead of the front in the non-ionized region at $z\to\infty$ has to be constant in time and as a consequence of (4) also constant in space:

$$\mathbf{E} = \begin{cases} E_\infty\ \hat{z} & z\to+\infty \\ 0 & z\to-\infty \end{cases}\ , \tag{8}$$

where $\hat{z}$ is the unit vector in z direction. For the boundary condition at $z\to-\infty$ we assumed that the ionized region behind the front extends to $-\infty$, screening the ionized bulk from the field. This implies, that a time independent amount of charge is traveling within the front, and no currents flow far behind the front in the ionized region.

For the further analysis, it is convenient to transform to a coordinate system $(x, y, \xi = z - vt)$ moving with velocity v in the z direction. Then the equations (2)–(4) read

$$\begin{aligned} \partial_t\sigma - v\partial_\xi\sigma \;&-\; (\rho-\sigma)\,\sigma + (\nabla\sigma)\cdot(\nabla\phi) - \sigma f(|\nabla\phi|) = 0\ , \\ \partial_t\rho - v\partial_\xi\rho \;&-\; \sigma f(|\nabla\phi|) = 0\ , \\ &\rho - \sigma + \nabla^2\phi = 0\ , \end{aligned} \tag{9}$$

where we expressed all quantities by electron density σ, ion density ρ and electric potential ϕ.

A front propagating uniformly with velocity v is a solution of (8), (9) where σ, ρ and ϕ depend of ξ only. With $\nabla\phi = \partial_\xi\phi\ \hat{z} = -E\ \hat{z}$, such a front solves

$$(v+E)\partial_\xi\sigma + (\rho-\sigma)\,\sigma + \sigma f(|E|) \;=\; 0\ , \tag{10}$$

$$v\partial_\xi\rho + \sigma f(|E|) \;=\; 0\ , \tag{11}$$

$$\rho - \sigma - \partial_\xi E \;=\; 0\ . \tag{12}$$

Now, for any non-vanishing far field E_∞, there is a continuous family of uniformly translating front solutions [12, 21], since the front propagates into an unstable state [18]. In particular, for $E_\infty > 0$ there is a solution for any velocity $v \geq 0$, and for $E_\infty < 0$, there is a solution for any $v \geq |E_\infty|$. These solutions are associated with an exponentially decaying electron density profile: an electron profile that asymptotically for large ξ decays like $\sigma(\xi) \propto e^{-\lambda\xi}$ with $\lambda \geq 0$, will propagate with velocity

$$v = -E_\infty + \frac{f(E_\infty)}{\lambda} \quad \text{in a field} \quad E_\infty < 0. \tag{13}$$

It will "pull" an ionization front along with the same speed. (For $E_\infty > 0$, the same equation applies for all $\lambda \geq f(E_\infty)/E_\infty$, hence for $v \geq 0$).

Dynamically, the velocity is selected by the initial electron profile [12, 18]. If initially the electron density strictly vanishes beyond a certain point ξ_0 (corresponding to $\lambda = \infty$ above)

$$\sigma = 0 = \rho \quad \text{for}\ \xi > \xi_0 \quad \text{at}\ t=0, \tag{14}$$

then this will stay true for all times $t > 0$ in a coordinate system moving with velocity

$$v = |E_\infty| \quad \text{for}\ E_0 < 0\ , \tag{15}$$

and the ionization shock front propagates precisely with the electron drift velocity $|E_\infty|$. In the remainder of the paper, we will consider this particular case.

C. Analytical front solutions

For future use, we now briefly recall the analytical solutions [12] of the uniformly translating fronts described by (10)–(12) and (8). The conservation $\partial_t q + \nabla \cdot \mathbf{j} = 0$ of charge $q = \rho - \sigma$ is contained in (2), (3), where the current $\mathbf{j}$ immediately can be identified with $\sigma\mathbf{E}$. Eq. (4) now allows in a standard way the identification of the total current

$$\partial_t \mathbf{E} + \sigma \mathbf{E} = \mathbf{j}_{tot} \quad , \quad \nabla \cdot \mathbf{j}_{tot} = 0. \tag{16}$$

For a planar front with constant and time independent field $\mathbf{E} = E_\infty \hat{z}$ (8) in the non-ionized region, the total current $\mathbf{j}_{tot} = j_{tot}(t)\hat{z}$ vanishes. In the comoving frame of Eqs. (9) and (10)–(12), this means

$$-v\partial_\xi E + \sigma E = 0 \tag{17}$$

for a uniformly translating front.

As already stated in [12], the front equations now reduce to two ordinary differential equations for σ and E

$$\begin{aligned} \partial_\xi[(v+E)\sigma] &= -\sigma f(E) \quad , \quad f(E) = |E|\alpha(E) \; , \\ v\partial_\xi \ln|E| &= \sigma, \end{aligned} \tag{18}$$

that can be solved analytically to give

$$\sigma[E] = \frac{v}{v+E}\,\rho[E], \tag{19}$$

$$\rho[E] = \int_{|E|}^{|E_\infty|} \frac{f(x)}{x}\,dx = \int_{|E|}^{|E_\infty|} \alpha(x)dx, \tag{20}$$

$$\xi_2 - \xi_1 = \int_{E(\xi_1)}^{E(\xi_2)} \frac{v+x}{\rho[x]}\,\frac{dx}{x}\;. \tag{21}$$

This gives us σ and ρ as functions of E, and the space dependence $E = E(\xi)$ implicitly as $\xi = \xi(E)$ in the last equation. It follows immediately from (21) that $E(\xi)$ is a monotonic function, and hence that the space charge $q = \rho - \sigma = \partial_\xi E$ has the same sign everywhere. According to (20), $\rho(\xi)$ is a monotonic function, too.

D. The negative ionization shock front

We now derive the particular properties of ionization fronts in negative fields $E_\infty < 0$ that emerge from an initial condition (14) where the electron density strictly vanishes beyond a certain point in space. These fronts propagate with the electron drift velocity $v = -E_\infty$. They carry a negative charge in the front region.

In contrast to all other uniformly translating fronts with $v > -E_\infty$, this front exhibits a discontinuity of the electron density at some point. We choose the coordinates such that the discontinuity is located at $\xi = 0$. The situation is shown in Fig. 1 for a uniformly translating front with velocity $v = |E_\infty|$ within a far field $E_\infty = -1$.

A discontinuity of σ means that $\partial_\xi \sigma$ is singular at this position. On the other hand, the expression $\sigma(\rho - \sigma + f(E))$ in Eq. (10) is finite or vanishing, therefore the product $(v+E)\partial_\xi\sigma$ in Eq. (10) may not diverge either.

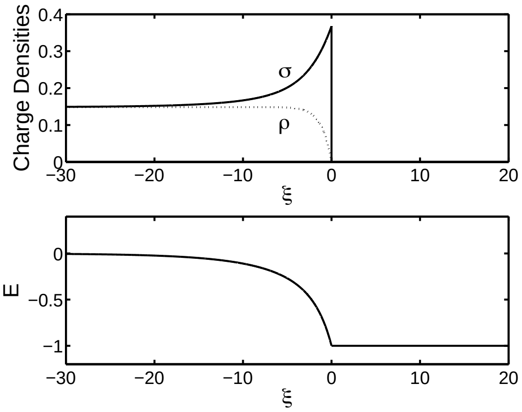

FIG. 1: Electron density σ (solid line in first plot), ion density ρ (dotted line in first plot) and electric field E (second plot) for a negative ionization shock front moving with $v = |E_\infty|$ in the comoving frame $\xi = z - vt$. The far field is $E_\infty = -1$.

Hence $(v+E)$ has to vanish at the position of the discontinuity, and therefore $E = E_\infty = -v$ at the position of the front. Furthermore, since $(v+E) \to 0$ for $\xi \uparrow 0$ while $\partial_\xi\sigma$ is bounded for $\xi < 0$ — as we will derive explicitly below in Eq. (29) — we have

$$\lim_{\xi \to 0} \Big[v + E(\xi)\Big]\,\partial_\xi \sigma = 0. \tag{22}$$

The fact that $\sigma(\xi)$ in Fig. 1 increases monotonically up to the position of the shock, is generic and can be seen as follows: according to (10), and since $(v+E) \geq 0$ and $\sigma \geq 0$, the sign of $\partial_\xi\sigma$ is identical to the sign of $\sigma - \rho - f(E)$. With the help of the exact solutions (19) and (20), with the definition of $f(E)$ in (5) and with identifying $v = |E_\infty|$, we find

$$\sigma - \rho - f(E) = |E| \int_{|E|}^{v} \frac{\alpha(x) - \alpha(E)}{v - |E|}\,dx \geq 0. \tag{23}$$

So $\sigma(\xi)$ increases monotonically as long as $\alpha(E)$ does the same. This is the case for Townsend form (6) or more generally for any $\alpha(E)$ that is monotonically increasing with E.

E. Asymptotics near the shock front

We now derive explicit expressions for $\sigma(\xi)$ etc. near the discontinuity. On approaching the position of the ionization shock front from below $\xi \uparrow 0$, the quantity

$$\epsilon = v + E = |E_\infty| - |E| \tag{24}$$

is a small parameter. The ion density (20) at this point can be expanded as

$$\rho[E] = \rho[v - \epsilon] = \alpha(v)\epsilon - \alpha'(v)\,\frac{\epsilon^2}{2} + O(\epsilon^3). \tag{25}$$

As the electron density is related to the ion density through $\sigma[E] = \rho[E]\, v/\epsilon$ according to (19), it is

$$\sigma[E] = v\alpha(v) - v\alpha'(v)\frac{\epsilon}{2} + O(\epsilon^2). \tag{26}$$

Eq. (21) evaluated for $E(\xi_2 = 0) = E_\infty < 0$ reads

$$-\xi = \int_{|E(\xi)|}^{v} \frac{v-x}{\rho[x]}\,\frac{dx}{x} = \int_0^{\epsilon} \frac{y}{\rho[v-y]}\,\frac{dy}{v-y}, \tag{27}$$

where in the last expression, the parameter ϵ (24) is introduced. Insertion of (25) now yields an explicit relation between ξ and E:

$$\begin{aligned} -\xi &= \frac{\epsilon}{v\alpha(v)} + O(\epsilon^2) \qquad (28)\\ \text{or}\quad \epsilon &= -v\alpha(v)\xi + O(\xi^2). \end{aligned}$$

Insertion of this approximately linear relation between ϵ and ξ into (25) and (26) together with the notation $f(v) = v\alpha(v)$ results in

$$\begin{aligned} \sigma(\xi) &= \theta(-\xi)\left(f(v) + \frac{f(v)\; v\; \alpha'(v)}{2}\;\xi + O(\xi^2)\right) && (29)\\ \rho(\xi) &= \theta(-\xi)\Big(-f(v)\;\alpha(v)\;\xi + O(\xi^2)\Big), && (30)\\ -E(\xi) &= v + \theta(-\xi)\Big(f(v)\;\xi + O(\xi^2)\Big), && (31) \end{aligned}$$

where we used $v = |E_\infty|$ and the step function $\theta(x)$, defined as $\theta(x) = 1$ or 0 for $x > 0$ or $x < 0$, respectively.

F. Asymptotics far behind the shock front

Far behind the front in the ionized region $\xi \to -\infty$, the asymptotic behavior of $\lim_{\xi\to-\infty}(\sigma,\rho,E) = (\sigma^-,\rho^-,E^-)$

$$\sigma^- = \rho^- = \int_0^v \alpha(x)\; dx \quad , \quad E^- = 0\;. \tag{32}$$

Expanding about this point as $\sigma(\xi) = \sigma^- + \sigma_1(\xi)$ etc., we derive in linear approximation

$$\partial_\xi \begin{pmatrix} \sigma_1 \\ \rho_1 \\ -E_1 \end{pmatrix} = \begin{pmatrix} \lambda & -\lambda & 0 \\ 0 & 0 & 0 \\ 1 & -1 & 0 \end{pmatrix} \cdot \begin{pmatrix} \sigma_1 \\ \rho_1 \\ -E_1 \end{pmatrix} \;, \tag{33}$$

with λ given by

$$\lambda = \frac{\sigma^-}{v} = \int_0^v \alpha(x)\;\frac{dx}{v}\;. \tag{34}$$

Two eigenvalues of the matrix in (33) vanish. The third eigenvalue of the matrix is the positive parameter λ, it produces the eigendirection

$$\begin{pmatrix} \sigma \\ \rho \\ -E \end{pmatrix}(\xi) \;=\; \begin{pmatrix} \sigma^- \\ \sigma^- \\ 0 \end{pmatrix} + A \begin{pmatrix} \lambda \\ 0 \\ 1 \end{pmatrix} e^{\,\lambda\xi} + O\left(e^{\,2\lambda\xi}\right)\;, \quad \text{for}\;\; \xi \to -\infty, \tag{35}$$

that describes the asymptotic solution deep in the ionized region. The free parameter $A > 0$ accounts for translation invariance.

G. Two degeneracies of the shock front

We have fixed the initial condition (14) and hence we have selected the front speed $v = -E_\infty$. Still there are two degeneracies remaining in the problem. The first one is the well known mode of infinitesimal translation that corresponds to the arbitrary position of the front. The second one is specific for the present problem and will play a role in the perturbation analysis in Sect. IV. It is the mode of infinitesimal change of far field E_∞. It corresponds to the arbitrariness of the field E_∞ in the non-ionized region with $\sigma = 0 = \rho$ ahead of the front and to the arbitrariness of the asymptotic ionization level $\sigma^- = \sigma = \rho$ behind the front where the field vanishes. To set the stage for the later analysis, the necessary properties of the modes are given.

An infinitesimal translation of the front in space generates the linear mode $(\sigma_t,\rho_t,E_t) = (\partial_\xi\sigma,\partial_\xi\rho,\partial_\xi E)$

$$\begin{aligned} (v+E)\partial_\xi\sigma_t &= \Big(2\sigma-\rho-f\Big)\sigma_t - \sigma\rho_t + \Big(\sigma f' - \partial_\xi\sigma\Big)E_t\\ v\partial_\xi\rho_t &= -f\sigma_t + \sigma f' E_t\\ \partial_\xi E_t &= \rho_t - \sigma_t \end{aligned} \tag{36}$$

with the definition $f' = \partial_x f(|x|)$, so that $f(E+E_t) = f - f'E_t + \ldots$ for $E < 0$. With the notation $\psi_t = -E_t$, the equations can be written in matrix form as

$$\partial_\xi \begin{pmatrix} \sigma_t \\ \rho_t \\ \psi_t \end{pmatrix} = \mathbf{N}_0(\xi)\cdot\begin{pmatrix} \sigma_t \\ \rho_t \\ \psi_t \end{pmatrix} \tag{37}$$

$$\mathbf{N}_0(\xi) = \begin{pmatrix} \dfrac{2\sigma-f-\rho}{v+E} & \dfrac{-\sigma}{v+E} & \dfrac{\partial_\xi\sigma-\sigma f'}{v+E} \\[2ex] \dfrac{-f}{v} & 0 & \dfrac{-\sigma f'}{v} \\[2ex] 1 & -1 & 0 \end{pmatrix} \tag{38}$$

Note that the matrix $\mathbf{N}_0(\xi)$ reduces to the matrix in Eq. (33) for $\xi \to -\infty$. The limiting value for $\xi \to 0$ is according to (29)–(31)

$$\begin{pmatrix} \sigma_t \\ \rho_t \\ \psi_t \end{pmatrix} \xrightarrow{\xi\uparrow 0} \begin{pmatrix} fv\alpha'/2 \\ -f\alpha \\ f \end{pmatrix}. \tag{39}$$

The second mode is generated by an infinitesimal change of the far field E_∞ and consecutively by an infinitesimal change of the velocity v. The discontinuity is taken at the position $\xi = 0$. In linear order, this variation creates a mode

$$\sigma_E(\xi) = \lim_{\epsilon\to 0}\frac{\sigma^{[E_\infty+\epsilon]}(\xi) - \sigma^{[E_\infty]}(\xi)}{\epsilon} \quad \text{etc.}, \tag{40}$$

that solves the inhomogeneous equation

$$\partial_\xi \begin{pmatrix} \sigma_E \\ \rho_E \\ \psi_E \end{pmatrix} = \mathbf{N}_0(\xi)\cdot\begin{pmatrix} \sigma_E \\ \rho_E \\ \psi_E \end{pmatrix} - \begin{pmatrix} \partial_\xi\sigma/(v+E) \\ \partial_\xi\rho/v \\ 0 \end{pmatrix}. \tag{41}$$

The inhomogeneity vanishes at $\xi \to -\infty$. Hence like the front solution itself and like the infinitesimal translation mode, also this mode has the eigendirection $(\delta\sigma^-, \delta\sigma^-, 0) + A\ (\lambda, 0, 1)\ e^{\lambda\xi} + \ldots$ asymptotically for $\xi \to -\infty$. The value of $\delta\sigma^-$ is given by $\delta\sigma^- = \partial\sigma^-/\partial|E_\infty| = \alpha(E_\infty)$ according to (32). For $\xi \uparrow 0$, the limiting values of the fields are

$$\begin{pmatrix} \sigma_E \\ \rho_E \\ \psi_E \end{pmatrix} \xrightarrow{\xi\uparrow 0} \begin{pmatrix} f' \\ 0 \\ 1 \end{pmatrix}, \tag{42}$$

which is the derivative of (29)–(31) with respect to v at $\xi = 0$.

III. SET-UP OF LINEAR STABILITY ANALYSIS

We now can proceed to study the stability of planar ionization shock fronts. The front propagates into the z direction. The perturbations have an arbitrary dependence on the transversal coordinates x and y. Within linear perturbation theory, they can be decomposed into Fourier modes. Therefore we need the growth rate $s(k)$ of an arbitrary transversal Fourier mode to predict the evolution of an arbitrary perturbation. Because of isotropy within the transversal (x, y)-plane, we can restrict the analysis to Fourier modes in the x direction, so we study linear perturbations $\propto e^{st+ikx}$. (The notation anticipates the exponential growth of such modes.) In the present section, we will derive the equations and the boundary conditions for the Fourier modes. In Sect. IV, we will solve them numerically and derive the analytical asymptotes (1).

A. Equation of motion

Any perturbation will also lead to a perturbation of the position of the ionization shock front. Because of the discontinuous nature of this front, it is convenient to formulate the perturbation theory within the coordinate system of the position of the perturbed shock front

$$\zeta = \xi - \delta\ e^{ikx+st}\ \ ,\ \ \xi = z - vt\ , \tag{43}$$

where z is the rest frame and ξ is the frame moving with the planar front. We write the perturbation as

$$\begin{aligned} \sigma(x,\zeta,t) &= \sigma_0(\zeta) + \delta\ \sigma_1(\zeta)\ e^{ikx+st}, \\ \rho(x,\zeta,t) &= \rho_0(\zeta) + \delta\ \rho_1(\zeta)\ e^{ikx+st}, \\ \phi(x,\zeta,t) &= \phi_0(\zeta) + \delta\ \phi_1(\zeta)\ e^{ikx+st}, \end{aligned} \tag{44}$$

where σ_0, ρ_0 and ϕ_0 are the electron density, ion density and electric potential of the planar ionization shock front from the previous section. Note, however, that these planar solutions are shifted to the position of the perturbed front. Substitution of these expressions into (9) gives to leading order in the small parameter δ

$$\begin{aligned} (v + E_0)\ \partial_\zeta\sigma_1 &= (s + 2\sigma_0 - \rho_0 - f)\ \sigma_1 \\ &\quad -\sigma_0\ \rho_1 + (\partial_\zeta\sigma_0 - \sigma_0 f')\ \partial_\zeta\phi_1 - s\partial_\zeta\sigma_0, \\ v\ \partial_\zeta\rho_1 &= -f\ \sigma_1 + s\ \rho_1 - \sigma_0 f'\ \partial_\zeta\phi_1 - s\partial_\zeta\rho_0, \\ \left(\partial_\zeta^2 - k^2\right)\ \phi_1 &= \sigma_1 - \rho_1 + k^2 E_0. \end{aligned} \tag{45}$$

Here $f = f(E_0)$, $f' = \partial_{|E|}f(|E|)\Big|_{E_0}$, and $E_0 = -\partial_\zeta\phi_0(\zeta)$ is the electric field of the uniformly translating front.

Note that these equations are not fully linear in $(\sigma_1, \rho_1, \phi_1)$, but contain the inhomogeneities $s\partial_\zeta\sigma_0$, $s\partial_\zeta\rho_0$ and k^2E_0. These inhomogeneities are generated by the choice of the coordinate ζ and would be absent in the coordinate system ξ of the unperturbed front. We choose the present notation where $\zeta = 0$ precisely coincides with the position of the discontinuity, since this makes the derivation of the boundary conditions at the shock front more comprehensible and also helps to identify the analytical solution for small k in Section V.B.

To elucidate the structure of Eq. (45), we drop all indices 0 and introduce the matrix notation

$$\partial_\zeta \begin{pmatrix} \sigma_1 \\ \rho_1 \\ \psi_1 \\ \phi_1 \end{pmatrix} = \mathbf{M}_{s,k} \cdot \begin{pmatrix} \sigma_1 \\ \rho_1 \\ \psi_1 \\ \phi_1 \end{pmatrix} - \begin{pmatrix} s\partial_\zeta\sigma/(v+E) \\ s\partial_\zeta\rho/v \\ -Ek^2 \\ 0 \end{pmatrix} \tag{46}$$

$$\mathbf{M}_{s,k}(\zeta) = \begin{pmatrix} \dfrac{s + 2\sigma - f - \rho}{v+E} & \dfrac{-\sigma}{v+E} & \dfrac{\partial_\zeta\sigma - \sigma f'}{v+E} & 0 \\ \dfrac{-f}{v} & \dfrac{s}{v} & \dfrac{-\sigma f'}{v} & 0 \\ 1 & -1 & 0 & k^2 \\ 0 & 0 & 1 & 0 \end{pmatrix} \tag{47}$$

Here we introduced the auxiliary field

$$\psi_1 = \partial_\zeta\phi_1, \tag{48}$$

that corresponds to the perturbation E_1 of the electric field, but with reversed sign.

B. Boundary conditions at the discontinuity

Having obtained the perturbation equations, we are now in the position to derive the boundary conditions. First we consider the boundary conditions at $\zeta = 0$. They arise from the boundedness of the electron density to the left of the shock front at $\zeta \uparrow 0$, and from the continuity of all other fields across the position $\zeta = 0$ of the shock front.

As discussed in Section II.D, for the uniformly propagating shock front, the quantity $(v + E)\ \partial_\zeta\sigma$ vanishes as

$\zeta \uparrow 0$, since $(v+E)$ vanishes and $\partial_\zeta \sigma$ is bounded. Since this should hold both for the full solution as well as for the unperturbed solution, it also holds for the perturbation

$$\lim_{\zeta \uparrow 0} \left[v + E(\zeta)\right] \partial_\zeta \sigma_1 = 0. \tag{49}$$

Furthermore

$$\left[v + E(\zeta)\right] \partial_\zeta \sigma_1 \equiv 0 \quad \text{for } \zeta \geq 0. \tag{50}$$

This identity is trivial for $\zeta > 0$, but nontrivial for $\zeta = 0$. Note that at this point, it is conceptually important to use the coordinate ζ rather than ξ, since it precisely marks the position of the discontinuity. When the explicit expressions (29)–(31) are inserted into (45), we find

$$\begin{aligned}(v+E)\partial_\zeta \sigma_1 &= \big(s + f(v)\big)\sigma_1 - f(v)\rho_1 - f(v)f'(v)\psi_1 \\ &\quad +(\psi_1 - s)\,\partial_\zeta \sigma + O(\zeta).\end{aligned} \tag{51}$$

First of all, $\partial_\zeta \sigma$ is singular at $\zeta = 0$, therefore (50) requires that its coefficient must vanish

$$\psi_1(0) = s \tag{52}$$

which gives the first boundary condition. Second, applying now (49) yields the second boundary condition

$$\big(s + f(v)\big)\sigma_1(0) - f(v)\rho_1(0) - f(v)f'(v)\psi_1(0) = 0. \tag{53}$$

Due to the discontinuity, actually two boundary conditions (52) and (53) result from (49) and (50).

In a second step the continuity of the other fields across $\zeta = 0$ is evaluated. The continuity of ρ we get from (11) and the fact, that σ and $|\mathbf{E}|$ are bounded for all ξ. It immediately yields the third boundary condition

$$\rho_1(0) = 0, \tag{54}$$

just like for the unperturbed equation. Finally, for the boundary conditions on field and potential, it is helpful that there is an exact solution for the non-ionized region at $\zeta > 0$ for a boundary with the harmonic form (43). Since ahead of the front there are no particles $\sigma = 0 = \rho$, there are also no space charges, and for the potential, one has to solve $\nabla^2 \phi = 0$ with the limit $\mathbf{E} = -\nabla\phi \to E_\infty\, \hat{\zeta} = -v\, \hat{\zeta}$ as $\zeta \to \infty$. The general solution is

$$\begin{aligned}\sigma &= 0 \\ \rho &= 0 \\ \phi &= v\xi + \delta\, c\, e^{-k\xi}\, e^{ikx+st} \qquad\qquad \text{for } \zeta > 0 \\ &= v\zeta + \delta(v + c\, e^{-k\zeta})\, e^{ikx+st} + O(\delta^2)\end{aligned} \tag{55}$$

with the yet undetermined integration constant c. Here we chose the gauge $\phi_0(\xi = 0) = 0$ for the unperturbed electric potential.

Now ϕ always is continuous, and $\mathbf{E} = -\nabla\phi$ is continuous, because the charge density $\rho - \sigma$ in (4) is non-infinite everywhere. The continuity of ϕ at $\zeta = 0$ implies

$$\phi_1(0) = v + c, \tag{56}$$

the continuity of $\partial_x \phi$ yields the same condition, and the continuity of $\partial_\zeta \phi$ implies

$$\psi_1(0) = -ck. \tag{57}$$

The five boundary conditions (52)–(54) and (56)–(57) determine the values of the four fields at $\zeta = 0$

$$\begin{pmatrix}\sigma_1\\ \rho_1\\ \psi_1\\ \phi_1\end{pmatrix} \xrightarrow{\zeta\uparrow 0} \begin{pmatrix} f'(v)\; s f(v)/(s+f(v)) \\ 0 \\ s \\ (vk - s)/k\end{pmatrix} \tag{58}$$

and the constant $c = -s/k$ in (55), hence the solution for the potential in the non-ionized region $\zeta > 0$ is

$$\begin{aligned}\sigma(x,\zeta>0,t) &= 0 = \rho(x,\zeta>0,t), \\ \phi(x,\zeta>0,t) &= v\zeta + \delta\, \frac{vk - s\, e^{-k\xi}}{k}\, e^{ikx+st}.\end{aligned} \tag{59}$$

C. Solution strategy and limits for $\zeta \to -\infty$

We aim to calculate the dispersion relation $s = s(k)$ for fixed k. For any s and k, the solution at $\zeta > 0$ is given explicitly by (59). This solution determines the value of the fields (58) at $\zeta = 0$ as a unique function of s and k. The expression (58) is the initial condition for the integration of (46) towards $\zeta \to -\infty$. The requirement that the solution approaches a physical limit at $\zeta \to -\infty$ has to determine s as a function of k. According to a counting argument, this is indeed the case, as will be explained now.

First, the limiting values of the fields at $\zeta = -\infty$ are comparatively easy: the total charge vanishes, hence σ_1 and ρ_1 approach the same limiting value $\sigma_1 \to \sigma_1^-$ and $\rho_1 \to \sigma_1^-$, and the electric field vanishes, hence $\psi_1 \to 0$ and $\phi_1 \to 0$. Here the limiting values at $\zeta \to -\infty$ again were denoted by the upper index $^-$ as in (35).

Second, the eigendirections are determined by linearizing the equations of motion (46) about this asymptotics. In a calculation similar to the one from Sect. II.F, one derives for $\zeta \to -\infty$

$$\begin{aligned}\begin{pmatrix}\sigma_1\\ \rho_1\\ \psi_1\\ \phi_1\end{pmatrix} \overset{\zeta\to-\infty}{\approx} &\begin{pmatrix}\sigma_1^-\\ \sigma_1^-\\ 0\\ 0\end{pmatrix} \\ &+ a_1\, e^{\lambda_1\zeta}\begin{pmatrix}\lambda_1^2 - k^2\\ 0\\ \lambda_1\\ 1\end{pmatrix} + a_2\, e^{\lambda_2\zeta}\begin{pmatrix}1\\ 1\\ 0\\ 0\end{pmatrix} \\ &+ a_3\, e^{k\zeta}\begin{pmatrix}0\\ 0\\ k\\ 1\end{pmatrix} + a_4\, e^{-k\zeta}\begin{pmatrix}0\\ 0\\ -k\\ 1\end{pmatrix}\end{aligned} \tag{60}$$

with the free parameters a_1, a_2, a_3, a_4 and σ_1^- and the eigenvalues

$$\lambda_1 = \frac{\sigma^- + s}{v} = \lambda + \lambda_2 \quad , \quad \lambda_2 = \frac{s}{v} \tag{61}$$

and λ from Eq. (34).

For positive s and k, all eigenvalues λ_1, λ_2 and k are positive except for the fourth one $-k$. Hence the first three eigendirections approach the appropriate limit for $\zeta \to -\infty$, while the fourth one does not. Therefore a solution can only be constructed for

$$a_4 = 0. \tag{62}$$

This condition determines the dispersion relation $s = s(k)$ when a solution of (46) and (58) is integrated towards $\zeta \to -\infty$.

IV. CALCULATION OF THE DISPERSION RELATION

Having set the stage, the dispersion relation is now first evaluated numerically for $E_\infty = -1$. Besides an expected result for small k, this investigation has delivered an previously unexpected result for large k. We were able to derive an analytical understanding of these results for arbitrary $E_\infty < 0$ which will be discussed after the numerical results.

A. Numerical results

The problem is to integrate the equations for the transversal perturbation (46) for fixed k and guessed s from the initial condition (58) at $\zeta = 0$ towards decreasing ζ. In general, the boundary condition (60) with (62) will not be met, so s has to be iterated until $a_4 \approx 0$. When the condition is met, the solution does not diverge for large negative ζ, otherwise it does. When passing through the appropriate $s = s(k)$, the sign of the divergence changes. This is how the data of Fig. 2 with their error bars were derived.

For the numerical integration, the ODEPACK collection of subroutines for solving initial value problems was used [22] to solve the seven ordinary differential equations for the unperturbed problem (10)–(12) and the perturbation (46)–(47) simultaneously. The unperturbed solution enters the matrix (47).

However, the numerics can not directly be applied to the problem in the form (46)–(47) because the matrix contains apparently diverging terms proportional to $1/(v + E)$ for $\zeta \to 0$. Therefore the behavior of the solution for $\zeta \to 0$ has to be evaluated in a similar way as in Sect. II.E. With the ansatz

$$\begin{aligned} \sigma_1(\zeta) &= \sigma_1(0^-) + C_1\zeta + O(\zeta^2) \ , \\ \rho_1(\zeta) &= \rho_1(0^-) + C_2\zeta + O(\zeta^2) \ , \\ \psi_1(\zeta) &= \psi_1(0^-) + C_3\zeta + O(\zeta^2) \ , \\ \phi_1(\zeta) &= \phi_1(0^-) + C_4\zeta + O(\zeta^2) \ , \end{aligned} \tag{63}$$

where $\sigma_1(0^-)$ etc. are given by (58), the parameters C_i become

$$\begin{aligned} C_2 &= -s\alpha \left(\frac{ff'}{s+f} + f + f' \right) \ , \\ C_3 &= s\left(-k + \frac{ff'}{s+f} \right) \ , \quad C_4 = s \ , \\ C_1 &= \frac{C_2 + (\alpha + v\alpha'/2)\, C_3 + s(v\alpha f'' + v\alpha' f'/2)}{2 + s/f} \end{aligned} \tag{64}$$

In the numerical procedure, the explicit solutions (29)–(31) and (63)–(64) are used until $\zeta = 10^{-5}$, then the differential equations are evaluated.

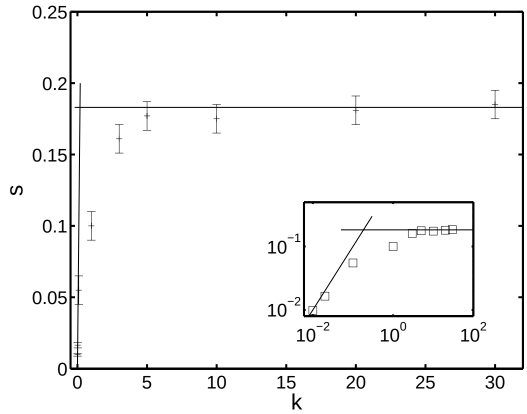

FIG. 2: Dispersion curve for $E_\infty = -1$, hence $v = 1$. The big figure shows the numerical data with error bars and the two analytical asymptotes for small and large k (lines). The inset shows the same data (squares) in double-logarithmic scale with the same two analytical asymptotes.

The numerical results for the dispersion relation in a field $E_\infty = -1$, i.e., for a shock front with velocity $v = 1$ are shown in Fig. 2. It can be seen that the dispersion curve for small k grows linearly, but then turns over and finally for large k saturates at a constant value.

B. Asymptotics for small k

We first derive the asymptotic behavior for small k for an arbitrary far field $E_\infty < 0$. It is $s(k) = vk + O(k^2)$ and shown in Fig. 2.

When the equations of motion (46) and (47) are evaluated up to first order in k, ϕ_1 decouples, and we get

$$\partial_\zeta \begin{pmatrix} \sigma_1 \\ \rho_1 \\ \psi_1 \end{pmatrix} = \mathbf{N}_s \cdot \begin{pmatrix} \sigma_1 \\ \rho_1 \\ \psi_1 \end{pmatrix} - \begin{pmatrix} s\partial_\zeta \sigma/(v+E) \\ s\partial_\zeta \rho/v \\ 0 \end{pmatrix} + O(k^2) \ , \tag{65}$$

where

$$\mathbf{N}_s(\zeta) = \begin{pmatrix} \dfrac{s+2\sigma-f-\rho}{v+E} & \dfrac{-\sigma}{v+E} & \dfrac{\partial_\zeta\sigma-\sigma f'}{v+E} \\ \\ \dfrac{-f}{v} & \dfrac{s}{v} & \dfrac{-\sigma f'}{v} \\ \\ 1 & -1 & 0 \end{pmatrix} + O(k^2) \tag{66}$$

is the truncated matrix $\mathbf{M}_{s,k}(\zeta)$ (47). The matrix $\mathbf{N}_s$ for $s=0$ reduces to the matrix $\mathbf{N}_0$ from Eq. (38) — this fact will be instrumental below. The fourth decoupled equation reads

$$\partial_\zeta\phi_1 = \psi_1 \tag{67}$$

The boundary condition (58) reduces to

$$\begin{pmatrix} \sigma_1 \\ \rho_1 \\ \psi_1 \end{pmatrix} \stackrel{\zeta\uparrow 0}{\longrightarrow} \begin{pmatrix} f'\ sf/(s+f) \\ 0 \\ s \end{pmatrix} + O(k^2) \tag{68}$$

and

$$\phi_1(0) = \frac{vk-s}{k}\ . \tag{69}$$

Now compare the mode $(\sigma_E, \rho_E, \psi_E)$ of infinitesimal change of far field E_∞ from Eqs. (40), (41) and (42) to the present perturbation mode in the limit of small k. After identifying

$$(\sigma_1, \rho_1, \psi_1) = (s\sigma_E, s\rho_E, s\psi_E), \tag{70}$$

the modes are identical up to contributions in the matrix and the boundary condition up to $O(s)$. In the limit $s \ll f(v) < v$, the two modes have to become identical. Integration over ψ_E yields for the electric potential $\phi_E(0) - \phi_E(-\infty) = \int_{-\infty}^0 dx\ \psi_E(x)$. This expression has to be of order unity since all other quantities are of order unity. But this implies that $\phi_1(0)$ due to (70) has to be of order s. Now compare the result for $\phi_1(0)$ in (69) which appears to depend in a singular way like $1/k$ on the small parameter k. But for small k and s the expression $(vk-s)/k$ indeed can be of order s: This requirement fixes the dispersion relation

$$s = vk + O(k^2) \quad \text{for} \quad k \ll \alpha(v)\ . \tag{71}$$

This result also has an immediate physical interpretation: $1/k$ is the largest length scale involved. It is much larger than the thickness of the screening charge layer. Therefore on the scale $1/k$, the charged front layer can be considered as an infinitesimally thin contribution along an interface line. The interface is equipotential since

$$\phi(x, \zeta=0, t) = \phi(0) + \delta\phi_1(0)\ e^{ikx+st} = 0 + O(k), \tag{72}$$

and the electric field ahead of the interface is

$$\mathbf{E}(x, \zeta=0^+, t) = -\big(v + \delta vk\ e^{ikx+st}\big)\ \hat{\zeta} + O(k^2) \tag{73}$$

according to (59). This field corresponds to an equipotential interface at position $\zeta = 0$, i.e., at a position

$$z = vt + \delta\ e^{ikx+st} \tag{74}$$

in the rest frame according to (43). When the interface moves with a velocity that equals the electron drift velocity $v = -E$, then a Fourier mode in the interface position (74) will grow precisely with the rate $s = vk$ from Eq. (71).

We conclude that a linear perturbation of the ionization front whose wave length is much larger than all other lengths, has the same evolution as a drifting equipotential line.

C. Asymptotics for large k

For large wave-vector k, the numerical results for the dispersion relation $s(k)$ in a field $E_\infty = -1$ approach a positive saturation value. We will now argue that the saturation value is given by $s(k) = f(E_\infty)/2$. This asymptotic value, which for $v=1$ equals $e^{-1}/2 = 0.184$, is included as a solid asymptotic line in Fig. 2.

When the electron and ion densities remain bounded, the equations with the most rapid variation in (46)–(47) for $k \gg 1$ are given by

$$\begin{aligned} \partial_\zeta\psi_1 &= k^2\phi_1 + k^2\ E(\zeta) + O(k^0), \\ \partial_\zeta\phi_1 &= \psi_1 \end{aligned} \tag{75}$$

On the short length scale $1/k$, the unperturbed electric field for $\zeta < 0$ can be approximated as in (31) by

$$E(\zeta) = -v - f(v)\zeta + O(\zeta^2), \tag{76}$$

so the equation for ϕ_1 becomes

$$\partial_\zeta^2\phi_1 = k^2\Big(\phi_1 - v - f(v)\zeta\Big). \tag{77}$$

The boundary condition (58) fixes $\phi_1(0) = (vk-s)/k$ and $\psi_1(0) = \partial_\zeta\phi_1 = s$. The unique solution of (77) with these initial conditions is

$$\phi_1(\zeta) = v + f(v)\zeta - \frac{f(v)}{2k}\ e^{k\zeta} + \frac{f(v)-2s}{2k}\ e^{-k\zeta} \tag{78}$$

for $\zeta < 0$. Now the mode $e^{-k\zeta}$ would increase rapidly towards decreasing ζ, create diverging electric fields in the ionized region and could not be balanced by any other terms in the equations. Therefore it has to be absent. The demand that its coefficient $(f(v)-2s)/2k$ vanishes, fixes the dispersion relation

$$s(k) = \frac{f(v)}{2} + O\left(\frac{1}{k}\right) \quad \text{for} \quad k \gg \alpha(v)\ . \tag{79}$$

Again there is a simple physical interpretation of this growth rate. The electric field is in leading order

$$\mathbf{E}(x,\zeta,t) = \begin{cases} -\hat{\zeta}\ \big(v + f(v)\zeta\big) + O(\delta) & \text{for} \quad \zeta < 0 \\ -\hat{\zeta}\ v + O(\delta) & \text{for} \quad \zeta > 0 \end{cases} . \tag{80}$$

When the discontinuity propagates with the local field $v = -E$, a perturbation in a field $\mathbf{E} = -\hat{\zeta}\big(v + E'\zeta\big)$ with slope $\partial_\zeta E = E'$ will grow with rate E'. The averaged slope of the field for $\zeta > 0$ and $\zeta < 0$ is $\partial_\zeta E = f(v)/2$, and this is precisely the growth rate (79) determined above.

V. CONCLUSIONS AND OUTLOOK

We have studied the (in)stability of planar negative ionization fronts against linear perturbations. Such perturbations can be decomposed into transversal Fourier modes. We have determined the dispersion relation $s = s(k)$ shown in Fig. 2 numerically for a fixed field $E_\infty = -1$ far ahead of the front, and we have derived the analytical asymptotes

$$s \;=\; \begin{cases} |E_\infty|\, k & \text{for } k \ll \alpha(|E_\infty|) \\ |E_\infty|\, \alpha(|E_\infty|)/2 & \text{for } k \gg \alpha(|E_\infty|) \end{cases} . \quad (81)$$

Since we have studied the minimal model, there is only one inherent length scale, namely the thickness of the charged layer as shown in Fig. 1. This thickness is approximated by $1/\alpha(E_\infty)$. The wave length $1/k$ of the Fourier perturbation therefore has to be compared with this single intrinsic length scale of the problem as done in (81).

A specific property of our calculation is the expansion about a discontinuity. Therefore we work in a coordinate system $\zeta = z - vt - \delta e^{ikx+st}$ (43) that precisely follows the position of the discontinuity, and we explicitly distinguish in all calculations the non-ionized region $\zeta > 0$ from the ionized region $\zeta < 0$. For the non-ionized region $\zeta > 0$, there is an exact analytical solution (59) for any s and k which determines the values of the fields at $\zeta = 0$ as given in (58). Eq. (58) serves as an initial condition for the integration towards $\zeta < 0$. The approach towards $\zeta \to -\infty$ according to (60) and (62) determines the growth rate s as a function of k. In general, this calculation has to be performed numerically with results as shown in Fig. 2. The limits of small and large k can be derived analytically. For small k, we can identify the perturbation mode with the mode of infinitesimal change of E_∞. For large k, the growth rate corresponds to the evolution of the discontinuity in the unperturbed electric field averaged across the discontinuity. Both limits therefore have a simple physical interpretation.

The aim of the work was to identify a regularization for the interfacial model as suggested in [8, 11] and treated in [10]. Indeed, we have found that a Fourier mode for large k in a far field $E_\infty = -v$ does not continue to increase with rate $s = vk$, but saturates at a value $s = f(v)/2$. Still this is a positive value, and whether this suffices to regularize the moving boundary problem, remains an open question.

Future work will have to investigate two questions. First of all, there is the "simple" possibility to extend the model by diffusion. Diffusion is certainly going to suppress the growth rate of Fourier modes with large k as our preliminary numerical work indicates. But there is also a second more subtle and interesting possibility: The growth rate of Fourier perturbations with large k could change for a curved front. After all, we have argued that the saturating growth rate $s = f(v)/2$ results from the average over the slope $-f(v)$ of the field in the ionized region and the slope 0 of the field in the non-ionized region. As for a curved front, the electric field in the non-ionized region will have a positive slope proportional to the local curvature, we expect the growth rate of a perturbation to decrease with growing curvature. These questions require future investigation.

Acknowledgments

M.A. gratefully acknowledges hospitality of CWI Amsterdam and a grant of the EU-TMR-network "Patterns, Noise and Chaos".

[1] W.J. Yi, P.F. Williams, J. Phys. D: Appl. Phys. **35**, 205 (2002).
[2] E.M. van Veldhuizen, W.R. Rutgers, J. Phys. D: Appl. Phys. **35**, 2169 (2002).
[3] L. Niemeyer, L. Pietronero, H.J. Wiesman, Phys. Rev. Lett. **52**, 1033 (1984).
[4] A.D.O. Bawagan, Chem Phys. Lett. **281** 325 (1997).
[5] V.P. Pasko, U.S. Inan, T.F. Bell, Geophys. Res. Lett. **28**, 3821 (2001).
[6] H. Raether, Z. Phys. **112**, 464 (1939) (in German).
[7] J.M. Meek, J.D. Craggs, *Electrical Breakdown in Gases* (Clarendon, Oxford, 1953).
[8] M. Arrayás, U. Ebert and W. Hundsdorfer, Phys. Rev. Lett. **88**, 174502 (2002).
[9] A. Rocco, U. Ebert, W. Hundsdorfer, Phys. Rev. E **66**, 035102 (2002).
[10] B. Meulenbroek, A. Rocco, U. Ebert, preprint: http://arxiv.org/abs/physics/0305112
[11] E.D. Lozansky and O.B. Firsov, J. Phys. D: Appl. Phys. **6**, 976 (1973).
[12] U. Ebert, W. van Saarloos and C. Caroli, Phys. Rev. Lett. **77**, 4178 (1996); and Phys. Rev. E **55**, 1530 (1997).
[13] A.A. Kulikovsky, Phys. Rev. Lett. **89**, 229401 (2002).
[14] U. Ebert, W. Hundsdorfer, Phys. Rev. Lett. **89**, 229402 (2002).
[15] U. Ebert and M. Arrayás, p. 270-282 in: *Coherent Structures in Complex Systems* (eds.: Reguera, D. *et al.*), Lecture Notes in Physics **567** (Springer, Berlin 2001).
[16] S.K. Dhali and P.F. Williams, Phys. Rev. A **31**, 1219 (1985) and J. Appl. Phys. **62**, 4696 (1987).
[17] P.A. Vitello, B.M. Penetrante, and J.N. Bardsley, Phys. Rev. E **49**, 5574 (1994).

[18] U. Ebert, W. van Saarloos, Phys. Rev. Lett. **80**, 1650 (1998); and Physica D **146**, 1-99 (2000).

[19] U. Ebert, W. van Saarloos, Phys. Rep. **337**, 139–156 (2000).

[20] Y.P. Raizer, *Gas Discharge Physics* (Springer, Berlin, 1991).

[21] A.N. Lagarkov, I.M. Rutkevich, *Ionization Waves in Electrical Breakdown in Gases* (Springer, New York, 1994).

[22] A.C. Hindmarsh, "ODEPACK, A Systematized Collection of ODE Solvers", p. 55-64 in: *Scientific Computing* (eds.: R.S. Stepleman *et al.*), IMACS Transactions on Scientific Computation, Vol. **1** (North-Holland, Amsterdam, 1983).